On dropsonde surface-adjusted winds and their use for the Stepped Frequency Microwave Radiometer wind speed calibration

Federica Polverari, Joseph W. Sapp, *Senior Member, IEEE*, Marcos Portabella, Ad Stoffelen, *Fellow, IEEE*, Zorana Jelenak, *Member, IEEE*, and Paul S. Chang, *Senior Member, IEEE*

***Abstract*—The airborne Stepped Frequency Microwave Radiometer (SFMR) provides measurements of 10-m ocean-surface wind speed in high and extreme wind conditions. These winds are calibrated using the surface-adjusted wind estimates from the so-called dropsondes. The surface-adjusted winds are obtained from layer-averaged winds scaled to 10-m altitude to eliminate the local surface variability not associated with the storm strength. The SFMR measurements and, consequently, the surface-adjusted dropsonde winds represent a possible reference for satellite instrument and model calibration/validation at high and extreme wind conditions. To this end, representativeness errors that those measurements may introduce need to be taken into account to ensure that the storm variability is correctly resolved in satellite retrievals and modelling. In this work, we compare the SFMR winds with the dropsonde surface-adjusted winds derived from the so-called WL150 algorithm, which uses the lowest 150-meter layer between 10 m to 350 m. We use nine years of data from 2009 to 2017. We focus on the effects of the layer altitude and thickness. Our analysis shows that the layer altitude has a significant impact on dropsonde/SFMR wind comparisons. Moreover, the averaged winds obtained from layers thinner than the nominal 150 m and closer to the surface are more representative of the SFMR surface wind speed than the WL150 speeds. We also find that the surface-adjusted winds are more representative of 10-km horizontally averaged SFMR winds. We conclude that for calibration/validation purposes, the WL150 algorithm can introduce noise and the use of actual 10-m dropsonde measurements should be further investigated.**

***Index Terms*—Calibration, dropsondes, ocean surface high and extreme wind reference, tropical cyclones, microwave radiometry.**

I. Introduction

Hurricanes and tropical cyclones are very dramatic phenomena as they are often associated with natural disasters, causing deaths and economic loss [1-3]. Designated aircrafts fly into the hurricanes in order to collect in-situ measurements of several atmospheric parameters. The Global Positioning System (GPS) dropwindsondes (hereafter referred to as dropsondes) are one of the instruments deployed from these aircrafts. They provide profiles of wind, humidity, pressure and temperature, as they descend until they reach the ocean surface [4]. In addition, these aircrafts are also equipped with Stepped Frequency Microwave Radiometers (SFMRs), which provide measurements of the 10-m surface wind speed and rain rate [5]. These measurements play a fundamental role in hurricane understanding and forecasting [6,7]. They are used as reference by the operational extreme wind community for the characterization of tropical and extra-tropical storms. They are also used in hurricane nowcasting applications.

The dropsonde 10-m surface-adjusted winds estimated from the dropsonde wind profiles are used instead of the actual dropsonde wind measured at an altitude of 10 m [8]. The dropsonde measurements close to the surface are considered as not reliable for hurricane intensity estimation. They can be compromised by local effects, such as long waves and wind

This work was supported in part by the Spanish R&D project L-BAND (ESP2017-89463-C3-1-R), which is funded by MCIN/AEI/10.13039/501100011033 and "ERDF A way of making Europe", and project INTERACT (PID2020-114623RB-C31), which is funded by MCIN/AEI/10.13039/501100011033. We also acknowledge funding from the Spanish government through the 'Severo Ochoa Centre of Excellence' accreditation (CEX2019-000928-S). This work is a contribution to CSIC PTI Teledetect. This work was also supported by the European Organization for the Exploitation of Meteorological Satellites (EUMETSAT), through the Tender 16_166-STC, under CHEFS Project EUM/CO/16/4600001953. Part of this work was also supported by an appointment to the NASA Postdoctoral Program at the Jet Propulsion Laboratory, California Institute of Technology, initially administered by Universities Space Research Association and now administered by Oak Ridge Associated Universities, under a contract with the National Aeronautics and Space Administration.

Federica Polverari was with the Institute of Marine Sciences, 08003 Barcelona, Spain. She is now a NASA Postdoctoral Program Fellow at the Jet Propulsion Laboratory, California Institute of Technology, Pasadena, CA 91109 USA (e-mail: federica.polverari@jpl.nasa.gov).

Joseph W. Sapp is with Global Science & Technology (GST), Inc., Greenbelt, MD 20770 USA, and also with the National Oceanic and Atmospheric Administration (NOAA)/National Environmental Satellite, Data, and Information Service (NESDIS) Center for Satellite Applications and Research (STAR), College Park, MD 20740 USA (e-mail: joe.sapp@noaa.gov).

Marcos Portabella is with the Institute of Marine Sciences, 08003 Barcelona, Spain (e-mail: portabella@icm.csic.es).

Ad Stoffelen is with the Royal Netherlands Meteorological Institute (KNMI), 3730 AE De Bilt, The Netherlands (e-mail: ad.stoffelen@knmi.nl).

Zorana Jelenak is with the National Oceanic and Atmospheric Administration (NOAA)/National Environmental Satellite, Data, and Information Service (NESDIS) Center for Satellite Applications and Research (STAR), College Park, MD 20740 USA, and also with the Cooperative Programs for the Advancement of Earth System Science (CPAESS), University Corporation for Atmospheric Research, Boulder, CO 80307 USA (e-mail:zorana.jelenak@noaa.gov).

Paul S. Chang is with the National Oceanic and Atmospheric Administration (NOAA)/National Environmental Satellite, Data, and Information Service (NESDIS) Center for Satellite Applications and Research (STAR), College Park, MD 20740 USA (e-mail: paul.s.chang@noaa.gov).

gusts so that they can introduce variability that is not associated with the storm strength. The surface-adjusted winds are also used as reference for the calibration and validation of the SFMR wind measurements [9, 10], although the spatial representations are quite different. In this manuscript, we investigate different spatial aggregations to determine the optimal dropsonde calibration reference for SFMR.

Recent works have analyzed the possibility to use the SFMR measurements as reference for the calibration of spaceborne instruments to sense high and extreme winds as well as for forward model derivation and validation [11-13]. However, when using SFMR to calibrate/validate other instruments and models at high and extreme wind conditions, this results in an indirect relationship with the dropsonde surface-adjusted winds. In this work, we mainly focus on the possible implications that the use of these surface-adjusted winds may have for calibration and validation purposes. It is crucial to take into account the possible errors between these estimates and SFMR winds in order to ensure that satellite retrievals and models accurately resolve the physical aspects of the hurricane variability [14]. The use of the surface-adjusted winds in nowcasting applications is not the scope of this work.

The dropsonde surface-adjusted wind estimates are obtained using layer-averaging techniques [15, 16] and in particular the so-called WL150 algorithm [8]. This algorithm consists of first the computation of an altitude-weighted average wind over 150 m, known as WL150 wind, obtained from the lowest 150-m layer of dropsonde measurements. Those measurements are generally collected within the altitude range from 10 m to 350 m. This averaged wind is then scaled to the surface to an altitude of 10 m using a scaling factor of about 0.85. This factor refers to layers of about 150 m thickness and at a mean altitude of about 85 m (hereafter referred to as nominal conditions). However, these nominal conditions do not always occur. The dropsondes can fail in reporting measurements at an altitude of 10 m, leading to involve layers at mean altitudes higher than the nominal 85 m. In addition, the presence of possible gaps of dropsonde readings within the nominal 150 m layer can lead to compute the WL150 wind using readings covering layers thinner than the 150 m thickness.

Our work aims to evaluate the WL150 algorithm when used for SFMR calibration/validation. To do that, we used nine years of data, that includes the surface-adjusted winds as well as the dropsonde wind profiles. We used these profiles to re-compute the WL150 winds and the surface-adjusted winds in nominal conditions, as well as by modifying the layer thickness and height. This allows us to determine the sensitivity of the WL150 algorithm to both these parameters and to understand the optimal representation for SFMR calibration. We find that lower layer height and shallower thickness provide a significant benefit for the correspondence between the SFMR and the dropsonde surface-adjusted wind speed.

The work is organized as follows. Section II describes the data sets used in this analysis. Section III.A describes the methodology used to collocate the SFMR and dropsonde winds. Sections III.B and III.C describe the methodology used to compute the dropsonde averaged wind with different layer altitudes and thicknesses, respectively. To analyze the WL150 algorithm, we first carried out a test to verify the accuracy of the 0.85 scaling factor using a logarithmic wind profile. The results are shown in Section IV.A. We then compared the WL150 wind at different layer altitudes with the corresponding dropsonde winds averaged in nominal conditions, as well as with the corresponding collocated SFMR surface winds. The results are given in Section IV.B. We subsequently evaluated the dropsonde winds averaged over layers with different widths with respect to the dropsonde 10-m surface wind measurements as well as with the collocated SFMR surface measurements. The results are provided in Section IV.C. In order to more thoroughly address the spatial representativeness differences between SFMR and dropsonde winds, an additional analysis has been carried out by comparing the 10-m surface-adjusted winds with the collocated SFMR winds at different spatial scales. The results are shown in Section IV.D. Finally, the conclusions are given in Section V.

II. Data sets

The SFMR and dropsonde datasets have been acquired by the many NOAA WP-3D and U.S. Air Force Reserve Command (AFRC) flights over several hurricane seasons. Nine years of data have been collected for this study, from 2009 to 2017.

A. SFMR Data

The SFMR is a C-band passive nadir-looking instrument built by ProSensing, Inc., Amherst, MA, USA [17]. It measures the ocean surface brightness temperature at six different frequencies from 4.55 to 7.2 GHz [5]. From these measurements both the 10-m surface wind speed and rain are estimated. The wind retrievals are available at a frequency sampling of 1 Hz.

These data have been reprocessed using a new Geophysical Model Function (GMF) [9]. This GMF was developed to correct a low bias in the SFMR wind speed retrievals between 15 and 45 m/s with respect to the surface-adjusted dropsonde wind speed. As explained in Sapp *et al*. [9], by using this new model in the SFMR retrieval algorithm the bias has been reduced by about 10%. Note that the precision of the SFMR wind speed retrievals below 15 m/s is considered as questionable due to the low sensitivity of the instrument to the physical processes at low wind conditions. The data products include a quality control (QC) flag to discriminate the valid solutions from those questionable or invalid. In this study we have only used the SFMR retrievals marked as valid solutions.

In terms of calibration accuracy, the SFMR dataset has also been inspected to ensure that the wind retrievals are good for instrument calibration. This consists of checking the accuracy of the corresponding brightness temperature measurements from the six different channels [11]. We further note that SFMR measures ocean surface properties, which depend on air mass density and stability [11,18]. These effects are ignored here and implicitly included in the calibration to 10-m winds.

B. GPS dropsonde data

The GPS dropsondes are instruments equipped with special sensors that provide several atmospheric measurements. In this study we focus on the wind speed measurements. According to Hock and Franklin [4], the vertical and horizontal wind components measured by the dropsondes are obtained from the

This article has been accepted for publication in IEEE Transactions on Geoscience and Remote Sensing. This is the author's version which has not been fully edited and content may change prior to final publication. Citation information: DOI 10.1109/TGRS.2022.3189310

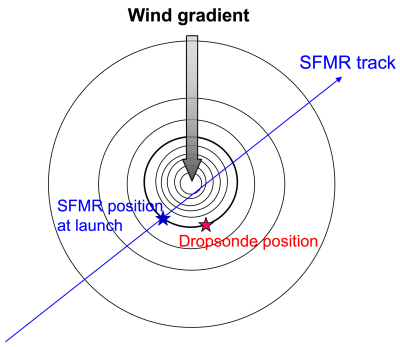

Fig. 1. Schematics of the SFMR/dropsonde wind collocation methodology.

dropsonde velocity components corrected by the acceleration resulting from the drag force. Both the dropsonde velocity and acceleration can be obtained by the dropsonde GPS-derived position measurements. The wind measurement accuracy ranges between 0.5-2 m/s with a vertical resolution of ~5 m.

We have collected the dropsonde wind speed profiles in both the raw and quality-controlled (QCed) formats. The QCed profiles were obtained by processing the raw profiles using the NCAR's Atmospheric Sounding Processing Environment (ASPEN) software, which systematically detects and removes the incorrect measurements. For the analysis of the WL150 algorithm, we have mainly used the QCed wind profiles. We used the raw profiles for retrieving the information of the dropsonde launch time, which is used for collocation purposes as explained in Section III. We notice that the QCed profiles report the dropsonde launch time as the time of the first reliable wind measurement, but this may not correspond to the actual launch time. Indeed, right after exiting the aircraft, the dropsonde sensors need time to settle in the new environmental conditions and during this time, they do not collect valid measurements. These measurements are filtered out by ASPEN so that they are removed from the QCed profiles.

In addition to the raw/QCed profiles, we have also collected the 10-m surface-adjusted winds obtained from the WL150 algorithm. Note that the whole data set only refers to the dropsondes outside the hurricane eyewall and in tropical cyclone conditions.

III. Methodology

Since the SFMR and the dropsonde winds have a different spatio-temporal resolution and sampling, we have first developed a collocation methodology to pair the SFMR wind measurements with the corresponding dropsonde. We have then computed the averaged WL150 wind with different configurations of the layer altitude and thickness. The details of the WL150 wind algorithm are given in the Appendix.

A. SFMR/dropsonde wind collocation

The dropsonde position at the surface is usually horizontally displaced with respect to the launch location. Such displacement is generally in the azimuthal direction with respect to the storm center. Since the storm wind gradient mostly changes in the radial direction, one can assume that the SFMR wind speed measured at the dropsonde launch time is representative of the surface wind conditions observed later by the dropsonde [11]. Therefore, for the SFMR/dropsonde wind comparison, we use the SFMR wind speed measurements at the dropsonde launch time to be paired with the corresponding dropsonde. A schematic of the SFMR/dropsonde wind collocation method is shown in Fig. 1.

Since more than one storm may simultaneously occur over different locations and more than one aircraft may be flying at the same day and time, to correctly pair the dropsonde and SFMR the correspondence of the aircraft name needs to be verified. The dropsonde profile products contain the sounding description which include the aircraft name. The SFMR product contains the aircraft identification, the so-called platform ID. However, while for the SFMR products from the NOAA-P3, the sounding description and the platform ID use the same name format to identify the aircraft, this is not the case for the AFRC flights, making the name verification agreement not straightforward. For this reason, we have used the following two criteria to pair the dropsonde/SFMR surface winds:

1) when the SFMR platform ID and the flight identification available in the sounding description match, the SFMR wind measurement whose time (t_{SFMR}) meets the following condition is selected:

$$\Delta t = |t_{SFMR} - t_{launch}| \leq 1 \text{ sec} \qquad (1)$$

Where t_{launch} is the dropsonde launch time. Note that since SFMR sampling rate is 1 sec and that the dropsonde time information is rounded to the nearest second, a Δt of 0 seconds should suffice. However, since that particular SFMR wind observation may be missing or QC-rejected, the collocation procedure allows the selection of the previous or consecutive SFMR measurement (i.e., at ± 1 second distance from t_{launch}), whichever is valid.

2) When the SFMR platform ID and the dropsonde flight identification do not match, an additional condition on the spatial distance is included in order to identify the corresponding SFMR platform, such that:

$$\Delta d = |d_{SFMR} - d_{launch}| \leq 10 \text{ km} \qquad (2)$$

where d_{SFMR} is the position of the selected SFMR point and d_{launch} is the dropsonde position corresponding to zero seconds after the launch. The seconds-after-launch value is stored in the dropsonde profile as a variable called $time_{offset}$. When the dropsonde position at $time_{offset} = 0$ s is not available, d_{launch} corresponds to the first available position at $time_{offset} > 0$ s.

Hereafter, we refer to the collocated SFMR wind at launch time as SFMR-L. A total of 1797 dropsondes have been collocated with SFMR; 31% of these collocations has been obtained with the additional condition shown in (2).

B. Assessing the impact of layer altitude and thickness

On the one hand, to assess the impact of the layer's altitude in the computation of the WL150 winds, we have fixed the layer thickness to be at least 100 m, allowing a gap of dropsonde readings up to 50 m at the top or at the bottom of the layer. This

This article has been accepted for publication in IEEE Transactions on Geoscience and Remote Sensing. This is the author's version which has not been fully edited and content may change prior to final publication. Citation information: DOI 10.1109/TGRS.2022.3189310

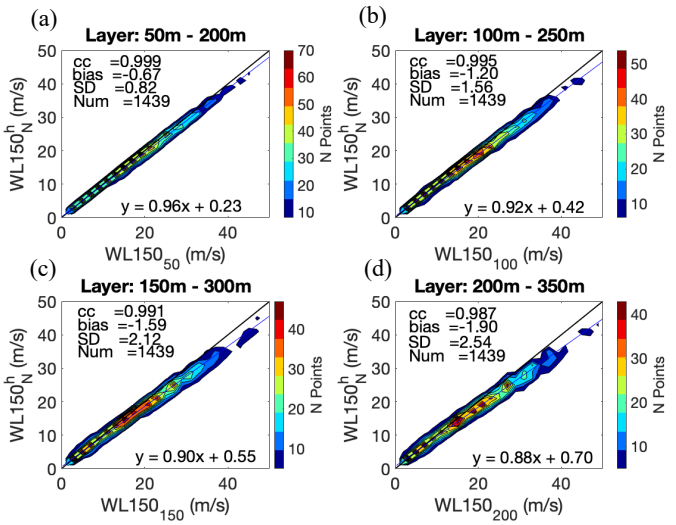

Fig. 2. Two-dimensional histograms of the dropsonde WL150 at different 150-m layer altitudes versus their corresponding $WL150_N{}^h$ (see colorbar). The 150-m layer is placed at 50-200m (a), 100-250m (b), 150-300m (c) 200-350m (d). The Pierson correlation coefficient (cc), bias, standard deviation (SD), and number of points (Num) can be found in the legend.

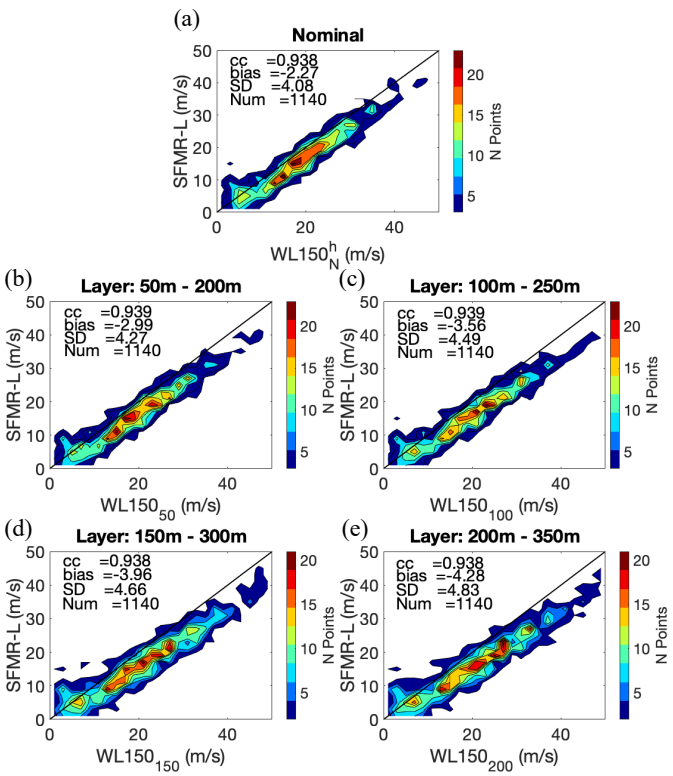

Fig. 3. Same as Fig. 2 but for SFMR-L instead of $WL150_N{}^h$. Note that (a) shows the comparison in nominal conditions.

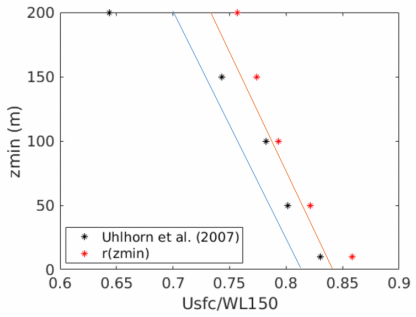

Fig. 4. Ratio of the dropsonde surface wind speeds and the WL150 wind speed, as a function of the altitude (red stars). The corresponding values of the ratio as presented in Uhlhorn *et al*., (2007) are also shown for comparison (black stars). For comparison, the corresponding ratios for a neutral profile with Z_0 = 1 mm (solid red) and 5 mm (solid blue) at 30 m/s 10-m wind speed.

is done to increase the dropsonde data available for this analysis. We have then computed the corresponding WL150 wind from layers at different mean altitudes. For this analysis, we have selected the dropsonde wind profiles which have at least five readings in each layer. Those profiles which do not provide a sufficient number of readings in each and all of the layers are discarded. This is done to ensure that the same dropsondes are used when moving the layer to higher altitudes and hence guarantee very similar weather variability conditions in the sample. Changing the altitude of the 150-m layer is intended to simulate dropsondes that fail in reporting measurements at different heights above the surface. To do that, we have changed the mean altitude such that the layer ranges between 50-200m, 100-250m, 150-300m and 200-350 m. We will refer to the corresponding WL150 wind as $WL150_{50}$, $WL150_{100}$, $WL150_{150}$ and $WL150_{200}$, respectively. The subscripts indicate the lowest altitude of the layer where we start to count the available dropsonde readings. The WL150 wind computed from a layer between 10-160 m, with a mean altitude of 85 m is considered here as the wind in nominal condition ($WL150_N{}^h$, where the superscript h indicates that it has been derived from the profiles selected to change the layer mean altitude).

In a second analysis, we have fixed the lowest altitude of the layer to be within 10 m to 15 m and we computed the wind by changing the layer thickness. This is intended to verify if the winds averaged over thinner layers close to the surface are more representative of SFMR sea surface wind measurements. We have set the wind in nominal conditions to have a layer thickness of 140-150 m ($WL150_N{}^w$, where the superscript w indicates that it has been derived from the profiles selected to change the layer thickness). We have then trimmed the layer to different thicknesses: 90-100m, 40-50m and 15-25m. We will refer to these winds as WL100, WL50 and WL25, respectively. The data have been filtered in such a way that the thinnest layer contains at least four dropsonde measurements. As for the previous case, those profiles which do not guarantee a sufficient number of readings at each layer are discarded. Although the $WL150_N{}^h$ and $WL150_N{}^w$ have been calculated with the dropsonde readings that meet the nominal criteria, note that these winds are not the same. They are the result of different filtering criteria; therefore, they are computed with different dropsonde readings.

IV. Results

A. Analysis using the logarithmic wind profile

Logarithmic wind profiles are commonly used to describe the distribution of winds with respect to altitude. They depend on the atmospheric stability, which refers to the stratification of the atmosphere near the surface. To verify the 0.85 scaling factor used in the WL150 algorithm, a profile under neutral stability conditions is assumed, so that the wind speed (U) with respect to the altitude (z) is modelled as [19,20]:

This article has been accepted for publication in IEEE Transactions on Geoscience and Remote Sensing. This is the author's version which has not been fully edited and content may change prior to final publication. Citation information: DOI 10.1109/TGRS.2022.3189310

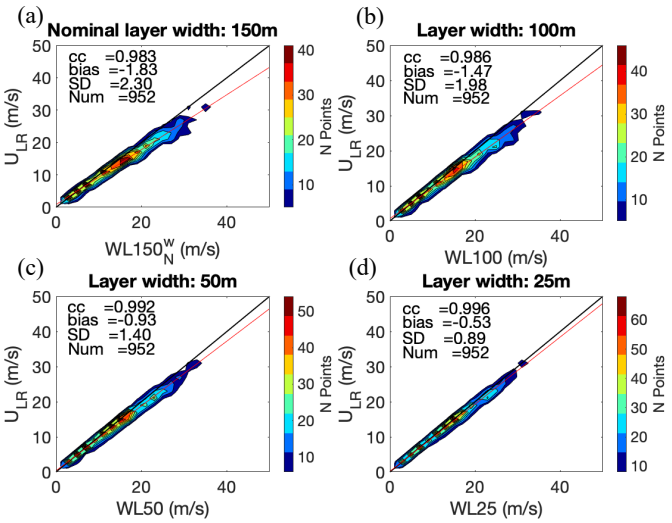

Fig. 5. Two-dimensional histograms (see color bar) of the dropsonde 10 m surface wind measurement and the dropsonde WL averaged winds at different layer thickness: (a) 145m-150m ($WL150_N{}^w$), (b) 95m-100m (WL100), (c) 45m-50m (WL50) and (d) 20m-25m WL25). All the layers correspond to the lowest altitude level, i.e., with a lowest reading around 10 m. The same statistical parameters as in Fig. 2 can be found in the legend.

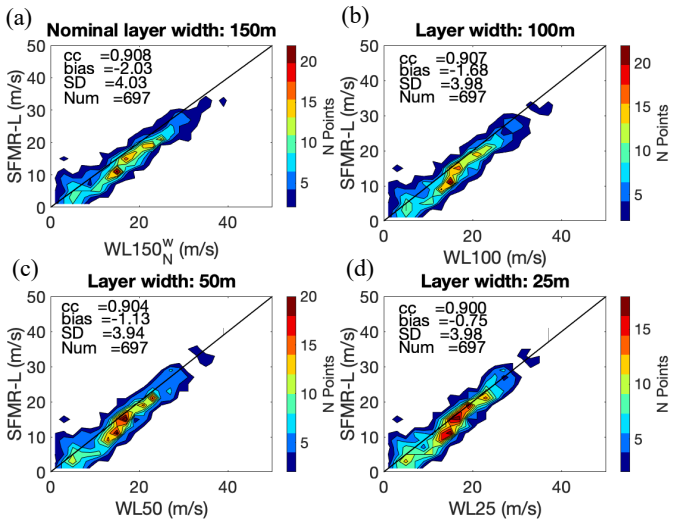

Fig. 6. Same as Fig. 5 but for SFMR-L instead of U_{LR}.

$$U(z) = \frac{u^*}{k}\ln\left(\frac{z}{Z_0}\right) \tag{3}$$

where u^* is the friction velocity, Z_0 is the roughness length and k is the Von Karman constant of ~0.41. The wind speed profile is computed assuming six dropsonde measurements at 10 m, 15 m, 45 m, 75 m, 105 m and 135 m. We have used two different configurations which correspond to a 10-m surface wind speed of about 30 m/s: (a) Z_0 = 5 mm and u^* = 1.58 m/s: (b) Z_0 = 1 mm and u^* = 1.30 m/s. These values represent a range of typical values in hurricane wind conditions. From these modelled profiles, we have derived the corresponding WL150 wind speed. The results of this test show that the ratio between the 10-m surface wind speed and the computed WL150 is 0.81 and 0.84 when using a logarithmic profile with assumptions (a) and (b), respectively. If scaling the WL150 wind to a wind speed at 15 m rather than at 10 m, the corresponding ratio is 0.85 and 0.87 for (a) and (b), respectively. Using a correction of 0.85 would imply a scaling to a wind speed at 15 m rather than 10 m, so a 5 m altitude error. This suggests that the scaling factor is very sensitive to the altitude of the dropsonde wind measurements and errors in the determination of this factor would lead to scale the winds at different altitudes rather than at 10 m from the surface.

B. Impact of the layer altitude

We have compared the $WL150_{50}$, $WL150_{100}$, $WL150_{150}$ and $WL150_{200}$ with the $WL150_N{}^h$. The two-dimensional histograms are shown in Fig. 2. For each histogram, we have computed the correlation coefficient (CC), the mean wind speed difference (bias) and the mean standard deviation of the wind speed differences (SD). The CC value decreases with increasing layer altitude. The absolute value of the bias (the SD) increases with altitude, going from 0.67 m/s (0.82 m/s) for the 50-200m layer to 1.90 m/s (2.54 m/s) for the 150-300m layer. A similar behavior is obtained with respect to the collocated SFMR-L surface wind speed. The results are shown in Fig. 3. The absolute value of the bias (the SD) goes from 2.27 m/s (4.03 m/s) for the lowest layer to 4.28 m/s (4.83 m/s) for the highest layer. Note that a bias between the $WL150_N{}^h$ and SFMR-L winds is expected since we are not using the dropsonde surface-adjusted winds (i.e., the scaling factor) in this comparison. As explained in Section IV.A, the wind speed increases approximately logarithmically with the altitude. Therefore, it is expected that the values of the WL150 wind speed increases when shifting the layer towards higher altitudes. However, note that this leads to larger differences between the WL150 and the SFMR-L winds.

According to Uhlhorn *et al*. [8] we have then defined the ratio between the 10-m surface winds and the WL150 wind as a function of the layer mean altitude (z), as described in (4). The results are shown in Fig. 4.

$$r(z) = 1 - 2.24\cdot 10^{-3}z + \\ +8.16\cdot 10^{-6}z^2 - 1.16\cdot 10^{-8}z^3 \tag{4}$$

The ratio tends to decrease as the altitude increases. Differences can be seen from this polynomial function and the ratio derived by Uhlhorn *et al.* [8], especially at high altitudes. Such differences may be due to the fact that in [8], only eyewall dropsondes were examined. The behavior in eyewall conditions has not been specifically addressed in this work.

In Fig. 4, the results using the logarithmic profile for both (a) and (b) assumptions are also shown. We can see a better agreement to $r(z)$ at 50 m and 100 m, when using the logarithmic profile with assumption (b). However, a less accurate fit at 10 m altitude is also seen. This might suggest uncertainty due to the dropsonde altitude, speed and acceleration knowledge.

C. Impact of the layer thickness

Figure 5 shows the comparison between the dropsonde wind speed measurement at the lowest layer altitude (U_{LR}- lowest reading) and the $WL150_N{}^w$, WL100, WL50 and WL25, along with the statistics as described in Section IV.B. As explained in Section III, the altitude of the lowest reading ranges between 10

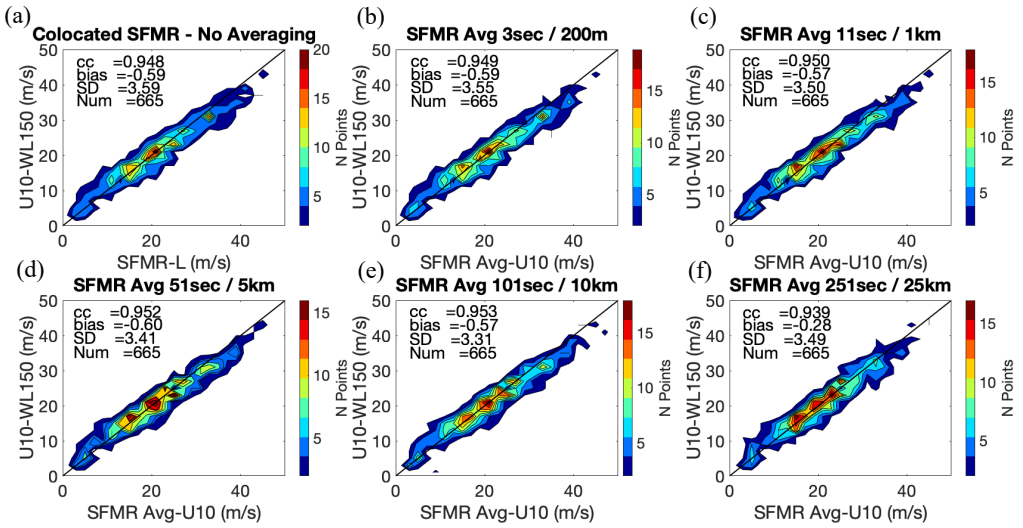

Fig. 7. Two-dimensional histograms (see colorbar) of the dropsonde 10-m winds estimated using the WL150 algorithm versus the along-track averaged SFMR 10-m winds at different temporal/spatial scales: nominal (a), 3sec/200m (b), 11sec/1km (c), 51sec/5km (d), 101sec/10km (e), 251sec/25km (f).

m to 15 m. When averaging the dropsonde measurements over thinner layers (w.r.t. the nominal 150-m layer) the CC between the measured U_{LR} and the averaged wind slightly increases, going from 0.983 for the nominal 150-m layer to 0.996 for th25-m layer. In addition, the bias and the SD significantly decrease when reducing the layer width to 25 m. The regression (red) line approaches the diagonal (black line) for decreasing layer thicknesses. These results suggest that the 25-m layer averaged winds are most representative of the dropsonde lowest level (10-m) winds, as expected, since an integrated measurement over a 25-m layer above the surface is enough to reduce the noise while it best represents the sea surface wind conditions. Similar results are obtained when comparing the different averaged winds and the collocated SFMR winds, as shown in Fig. 6. The CC value remains high and does not significantly change. The SD values slightly decrease from 4.03 (with respect to $WL150_N{}^w$), to 3.98 (with respect to WL25). On the other hand, the bias considerably decreases from -2.03 m/s to -0.75 m/s.

D. Representativeness error at different SFMR spatial scales

SFMR and dropsonde winds are indeed integrated measurements but represent different spatial and temporal scales. In order to compare them, one should first assess the different spatial and temporal representation of both sources. One way to do this is by computing SFMR along-track averages, centered at the SFMR-L position, over 3 sec, 11 sec, 51 sec, 101 sec and 251 sec. We have assumed an aircraft speed of about 100 m/s on average, so that such temporal distances correspond to a spatial distance of 200 m, 1 km, 5 km, 10 km and 25 km, respectively. In order to consistently compute averaged winds, we have set a limit for the minimum number of QC-accepted SFMR points used to compute the average. Since the SFMR winds are provided at 1 Hz, this threshold is set to 2 points, 9 points, 40 points, 80 points and 200 points, respectively (i.e., a minimum of about 80% of valid points, except for the 3-sec averages for which a minimum of 66% of valid points is required). About 37% of the available collocations have a corresponding SFMR flight that meets these constraints. The results in Fig. 7 show that the SFMR winds at different temporal/spatial scales are in relatively good agreement with the dropsonde surface adjusted winds. On the one hand, there is a slight decrease of the SD as well as an increase of the CC for increased spatio-temporal averaging, up to 10 km resolution. On the other hand, the SD (CC) increases (decreases) for the 25-km averaged winds. This suggests that the dropsonde estimated surface winds obtained by the WL150 algorithm may be representative of 10-km averaged SFMR winds. Note that the location difference between SFMR and dropsonde, as explained in Section III.A, may increase the differences seen in SD and CC at the 5-km scales and smaller, as these scales are not resolved in the collocation (see Fig. 1).

V. Conclusions

The operational high and extremes wind community rely on the dropsonde-derived surface-adjusted winds as reference for hurricane nowcasting. In-situ 10-m winds from dropsondes are also needed for instrument calibration and weather model validation, directly or indirectly. However, current dropsonde winds are estimated from the dropsonde wind profiles using the WL150 algorithm, so that their accuracy and representativeness remains an open issue and further investigations are required for calibration/validation purposes.

In this work we evaluate the WL150 algorithm with respect to the SFMR winds. We found that when averaging the dropsonde readings over a layer at mean altitudes higher than the nominal 85 m, the resulting WL150 wind increases. This leads to higher biases and standard deviations with respect to the nominal WL150 wind as well as to the collocated SFMR surface wind. Such bias is not constant and it appears rather scaled with respect to the wind speed. In order to properly scale the WL150 wind to the 10-m height, the scaling factor used in the WL150 algorithm needs to consider the corresponding mean layer altitude. Our analysis also shows that, when averaging the dropsonde readings over a much thinner layer

than the nominal 150-m layer close to the surface, the bias and the standard deviation between the averaged winds and the corresponding lowest dropsonde reading are significantly reduced. Similar conclusions are drawn when comparing the averaged dropsonde readings with the collocated SFMR wind. This suggests that the winds averaged over 25-m rather than 150-m layers are more representative of the 10-m winds. We also found that the dropsonde surface-adjusted winds are more representative of 10-km horizontally averaged SFMR winds than of single closest collocated winds, which is partly explained by the average closest collocation distance.

We conclude that the WL150 winds can introduce noise and biases when converted into 10-m surface winds. The actual dropsonde 10-m winds might represent a more direct calibration and validation resource for SFMR, satellite instruments and weather models. However, the actual dropsonde winds are computed from the dropsonde velocity and acceleration caused by the drag force. This information is obtained from the GPS-derived dropsonde position time series [4]. The position computation by the dropsonde GPS chip has not been investigated yet, nor its derivation of speed and acceleration, which may cause further bias. That information appears essential to understand and characterize the possible errors and the error propagation near the surface, when the sonde is strongly decelerating. Therefore, the accuracy and reliability of the dropsonde actual 10-m winds still remain an open issue and additional analysis using logarithmic wind profiles should be considered for further investigations.

APPENDIX

THE WL150 ALGORITHM

According to Sapp *et al.* [9], the WL150 wind can be computed from the WL150 zonal (u_{L150}) and meridional (v_{L150}) components. They are obtained from the components of the dropsonde wind samples available within the layer, as described in (5) and (6), respectively:

$$u_{L150} = \frac{\sum_{i=1}^{n} u_i w_i}{h_n - h_1} \tag{5}$$

$$v_{L150} = \frac{\sum_{i=1}^{n} v_i w_i}{h_n - h_1} \tag{6}$$

Where n is the number of dropsonde wind samples in the 150m-layer, u_i and v_i are the sample i zonal and meridional components, respectively. The w_i are the corresponding weights computed from each sample altitude h_i, as shown in (7) and (8). A continuous distribution of the wind samples within the layer is normally assumed.

$$w_1 = \frac{h_2 - h_1}{2};\ w_n = \frac{h_n - h_{n-1}}{2}; \tag{7}$$

$$w_i = \left[\left(\frac{h_{i+1} - h_i}{2} + h_i\right) + -\left(\frac{h_i - h_{i-1}}{2} + h_{i-1}\right)\right];\ i = 2, \dots, n-1 \tag{8}$$

In order to convert the WL150 wind components into the corresponding 10m-surface wind components, a factor of 0.85 is generally applied to u_{L150} and the v_{L150}, as shown in (9) and (10) [8],

$$u10_{WL150} = 0.85u_{L150} + 0.89 \tag{9}$$

$$v10_{WL150} = 0.85v_{L150} + 0.89 \tag{10}$$

From the wind components, then the corresponding dropsonde 10m-surface wind speed and direction is estimated. Another possible approach is to apply the WL150 algorithm directly to the wind speed measurements rather than to the wind components. This is accurate in terms of estimating the wind speed, but it can bring some uncertainty in the estimation of the surface wind direction.

ACKNOWLEDGEMENT

The views, opinions, and findings in this report are those of the authors and should not be construed as an official NOAA or U.S. government position or policy.

REFERENCES

[1] L. Bevere, I. Fan, T. Holzheu, "Swiss Re Institute estimates USD 83 billion global insured catastrophe losses in 2020, the fifth-costliest on record", Accessed: Nov. 9 2021. [Online]. Available: https://www.swissre.com/media/news-releases/nr-20201215-sigma-full-year-2020-preliminary-natcat-loss-estimates.html

[2] J. L Beven *et al*., "Atlantic Hurricane Season of 2005", *Monthly Weather Review*, vol. 136, no. 3, pp. 1109-1173, 2008. Accessed: Nov 10, 2021, [Online]. Available: https://journals.ametsoc.org/view/journals/mwre/136/3/2007mwr2074.1.xml

[3] E. Blake, C. Landsea, E. J. Gibney, "The Deadliest, Costliest, and Most Intense United States Tropical Cyclones From 1851 to 2010 (and Other Frequently Requested Hurricane Facts)", National Hurricane Center, Miami, FL., NOAA Tech Memo., NWS NHC-6, 2011. Accessed: Nov. 10, 2021. [Online]. Available: https://www.nhc.noaa.gov/pdf/nws-nhc-6.pdf.

[4] T. F. Hock, and J. L Franklin, "The NCAR GPS dropwindsonde," *Bull. Amer. Meteor. Soc.*, vol. 80, no. 3, pp. 407–420, 1999.

[5] E. W. Uhlhorn, and P. G. Black, "Verification of Remotely Sensed Sea Surface Winds in Hurricanes," *J. of Atmos. and Ocean. Technol*., vol. 20, no. 1, pp 99-116, 2003

[6] E. N. Rappaport *et al.*, "Advances and Challenges at the National Hurricane Center", *Weather and Forecasting*, vol. 24, no. 2, pp. 395-419, 2009. Accessed: Nov 10, 2021. [Online]. Available: https://journals.ametsoc.org/view/journals/wefo/24/2/2008waf2222128_1.xml

[7] R. Rogers *et al*., "The Intensity Forecasting Experiment: A NOAA Multiyear Field Program for Improving Tropical Cyclone Intensity Forecasts", *Bulletin of the American Meteor. Soc.*, vol. 87, no. 11, pp. 1523-1538, 2006. Accessed: Nov 10, 2021. [Online]. Available: https://journals.ametsoc.org/view/journals/bams/87/11/bams-87-11-1523.xml

[8] E. Uhlhorn, P. Black, J. Franklin, M. Goodberlet, J. Carswell and A. Goldstein, "Hurricane Surface Wind Measurements from an Operational Stepped Frequency Microwave Radiometer", *Mon. Weather Rev.,* vol. 135, p. 3070–3085, 2007

[9] J. W. Sapp, S.O. Alsweiss, Z. Jelenak, P.S. Chang, J. Carswell, "Stepped Frequency Microwave Radiometer Wind-Speed Retrieval Improvements,"*Remote Sensing,* vol. 11, no. 214, 2019.

[10] B. Klotz and E. Uhlhorn, "Improved Stepped Frequency Microwave Radiometer Tropical Cyclone Surface Winds in Heavy Precipitation", *J. Atmos. Ocean. Technol.,* vol. 31, no. 11, p. 2392–2408, 2014.

[11] A. Stoffelen *et al.*, "C-band high and extreme-force speeds (CHEFS)," EUMETSAT, Darmstadt, Germany, CHEFS Final Project Rep. EUMETSAT ITT 16/166, 2020.

[12] F. Polverari, M. Portabella, W. Lin, J. W. Sapp, A. Stoffelen, Z. Jelenak, P.S. Chang, "On High and Extreme Wind Calibration Using ASCAT," *IEEE Trans. Geosci. Remote Sens*. 2021. doi: 10.1109/TGRS.2021.3079898

[13] A. Mouche, B. Chapron, J. Knaff, Y. Zhao, B. Zhang, C. Combot, "Copolarized and cross-polarized SAR measurements for high-resolution description of major hurricane wind structures: Application to Irma category 5 hurricane," *J. of Geophys. Res.: Oceans*, vol. 124, no. 6, pp. 3905– 3922, 2019. doi: https://doi.org/10.1029/2019JC015056

[14] A. Stoffelen, G.-J. Marseille, W. Ni, A. Mouche, F. Polverari, M. Portabella, W. Lin, J. W. Sapp, P. S. Chang, Z. Jelenak, "Hurricane Ocean Wind Speeds," *in Proc. IEEE Int. Geosci. and Remote Sens. Symposium. IGARSS*, 2021, Brussels, Belgium (Virtual meeting), pp. 1182-1185. doi: 10.1109/IGARSS47720.2021.9554667.

[15] J. L. Franklin, M. L. Black, K. Valde, "GPS Dropwindsonde Wind Profiles in Hurricanes and Their Operational Implications", *Weather Forecast,* vol. 18, pp. 32–44, 2003.

[16] J. W. Sapp, S.O. Alsweiss, Z. Jelenak, P. S. Chang, S. J. Frasier, J. Carswell, "Airborne Co-Polarization and Cross-Polarization Observations of the Ocean-Surface NRCS at C-Band," *IEEE Trans. Geosci. Remote Sens*., vol. 54, no. 10, pp. 5975–5992, 2016.

[17] *Stepped Frequency Microwave Radiometer (SFMR)-ProSensing*. Accessed: Nov. 9, 2021. [Online]. Available: https://www.prosensing.com/crb-product/sfmr.

[18] J. de Kloe, A. Stoffelen and A. Verhoef, "Improved Use of Scatterometer Measurements by Using Stress-Equivalent Reference Winds", IEEE Journal of Selected Topics in Applied Earth Observations and Remote Sensing, vol. 10, no. 5, pp. 2340-2347, May 2017, doi: 10.1109/JSTARS.2017.2685242.

[19] M. D., Powell, P. J. Vickery, T. A. Reinhold, "Reduced drag coefficients for high wind speeds in tropical cyclones," *Nature*, vol. 422, pp. 279–283, 2003.

[20] A. B. Kara, A. J. Wallcraft, M. A. Bourassa, "Air-sea stability effects on the 10 m winds over the global ocean: Evaluations of air-sea flux algorithms", *J. Geophys. Res.*, vol. 113, no. C04009, 2008. doi:10.1029/2007JC004324

Federica Polverari received the M.Sc. degree in electronic engineering and the Ph.D. degree in the Information and Communications Technologies–Radar and Remote Sensing from the Sapienza University of Rome, Rome, Italy, in 2013 and 2017, respectively.

From 2017 to 2019 she was a Postdoctoral Researcher in radar scatterometry, at the Institut de Ciències del Mar, Barcelona, Spain. In 2019 she was awarded a NASA Postdoctoral Program Research Fellowship at NASA Jet Propulsion Laboratory, California Institute of Technology, Pasadena, CA, USA. Her research interests include active microwave remote sensing of ocean surface winds with focus on the characterization of extreme wind retrieval capabilities of spaceborne scatterometry using airborne radiometry and in-situ wind measurements, scatterometer geophysical model function development, modeling and characterization of the ocean surface scatterometer response.

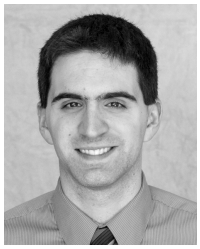

Joseph W. Sapp (Senior Member, IEEE) received the B.S. degree in electrical engineering from The Pennsylvania State University, University Park, PA, USA in 2006, and the Ph.D. degree in electrical and computer engineering from the University of Massachusetts Amherst, Amherst, MA, USA, in 2015.

From 2006 to 2009, he was a Project Electrical Engineer with Lutron Electronics Company, Inc., Coopersburg, PA, USA, during which he was involved in the embedded software design of multiple commercial products. In 2009, he joined the Microwave Remote Sensing Laboratory, University of Massachusetts Amherst, to complete his graduate work. During this time, he had the opportunity to begin participating in flights with the National Oceanic and Atmospheric Administration (NOAA) Hurricane Hunters. Since 2015, he has been with NOAA/National Environmental Satellite, Data, and Information Service (NESDIS)/Center for Satellite Applications and Research (STAR), College Park, MD, USA, as a Support Scientist with Global Science and Technology, Inc., Greenbelt, MD, USA. His recent research involves using active, passive, and in situ sensors together to improve the algorithms and equipment used in remote sensing of ocean surface and atmospheric wind vectors in extreme environments

Marcos Portabella was born in Barcelona, Spain, in 1970. He received the B.Sc. degree in physics from the University of Barcelona, Barcelona, Spain, in 1994, the M.Sc. degree in remote sensing from the Institute of Space Studies of Catalonia, Barcelona, in 1995, and the Ph.D. degree in physics from the University of Barcelona.

He is currently with the Institut de Ciències del Mar, Barcelona, Spain, where he is involved in satellite remote sensing, and particularly scatterometry and L-band radiometry.

Ad Stoffelen (Senior Member, IEEE) received the M.Sc. degree in physics from the Technical University of Eindhoven, Eindhoven, The Netherlands, in 1987, and the Ph.D. degree in meteorology on scatterometry from the University of Utrecht, Utrecht, The Netherlands, in 1998. He currently leads a Group on active satellite sensing with the Royal Netherlands Meteorological Institute, De Bilt, The Netherlands, where he is involved in the future missions and research and development of retrieval to 24/7 operations, numerical weather prediction (NWP) mesoscale wind data assimilation, user training, and services. He is also with the European Space Agency Doppler Wind Lidar Mission—Aeolus—on atmospheric dynamics. His research interests include establishing an international scatterometer virtual constellation.

Zorana Jelenak (Member, IEEE) received the Ph.D. degree in physics from the Waikato University, Hamilton, New Zealand, in 2000.

In March 2001, she joined the Ocean Winds Team, National Oceanic and Atmospheric Administration (NOAA)/National Environmental Satellite, Data, and Information Service (NESDIS)/Office of Research Applications (ORA), as a University Corporation for Atmospheric Research (UCAR) Visiting Scientist. She is a member of the NASA Ocean Surface Winds Science Team, a NOAA's Environmental Data Record (EDR) Algorithm Lead for the AMSR-2 radiometer, and a member of the NASA CYGNSS Science Team. Her interests are in ocean surface wind vector measurements from active and passive microwave measurements and its applicability in an operational near-real time environment, retrieval algorithm development, model function development, advanced statistical analysis, and error analysis for improved algorithm characterization.

Paul S. Chang (Senior Member, IEEE) received the B.S. degree in electrical engineering from the Union College, Schenectady, NY, USA, in 1988, and the Ph.D. degree in electrical engineering from the University of Massachusetts Amherst, Amherst, MA, USA, in 1994.

Since 1994, he has been a Research Physical Scientist with the Center for Satellite Applications and Research, National Environmental Satellite, Data and Information Service (NESDIS), National Oceanic and Atmospheric Administration (NOAA). Current activities include research and development in active and passive microwave remote sensing of the ocean surface with an emphasis on retrieval of the ocean surface wind field. Wind retrieval algorithm improvements and new product developments are pursued through the analyses of satellite and aircraft microwave remote sensing data. An emphasis is placed on transitioning research results into operational use, which involves cooperative relationships with the operational facets of NESDIS and with the National Weather Service, a primary end user of these data. Current efforts are focused on working on the METOP-ASCAT, SCATSAT, CFOSAT, CYGNSS, and GCOM-W missions in addition to planning and risk reduction activities for future ocean vector winds missions.